

Spectral Polynomial Chaos Solutions of the Stochastic Advection Equation

M. Jurdak, C.-H. Su and G.E. Karniadakis*
Division of Applied Mathematics
Brown University

October 29, 2001

Abstract

We present a new algorithm based on Wiener-Hermite functionals combined with Fourier collocation to solve the advection equation with stochastic transport velocity. We develop different strategies of representing the stochastic input, and demonstrate that this approach is orders of magnitude more efficient than Monte Carlo simulations for comparable accuracy.

Key Words: Stochastic differential equations, Wiener-Hermite expansions, Polynomial Chaos, Uncertainty

*Corresponding author, gk@cfm.brown.edu

Report Documentation Page

Form Approved
OMB No. 0704-0188

Public reporting burden for the collection of information is estimated to average 1 hour per response, including the time for reviewing instructions, searching existing data sources, gathering and maintaining the data needed, and completing and reviewing the collection of information. Send comments regarding this burden estimate or any other aspect of this collection of information, including suggestions for reducing this burden, to Washington Headquarters Services, Directorate for Information Operations and Reports, 1215 Jefferson Davis Highway, Suite 1204, Arlington VA 22202-4302. Respondents should be aware that notwithstanding any other provision of law, no person shall be subject to a penalty for failing to comply with a collection of information if it does not display a currently valid OMB control number.

1. REPORT DATE 29 OCT 2001		2. REPORT TYPE		3. DATES COVERED 00-10-2001 to 00-10-2001	
4. TITLE AND SUBTITLE Spectral Polynomial Chaos Solutions of the Stochastic Advection Equation				5a. CONTRACT NUMBER	
				5b. GRANT NUMBER	
				5c. PROGRAM ELEMENT NUMBER	
6. AUTHOR(S)				5d. PROJECT NUMBER	
				5e. TASK NUMBER	
				5f. WORK UNIT NUMBER	
7. PERFORMING ORGANIZATION NAME(S) AND ADDRESS(ES) Brown University, Division of Applied Mathematics, 182 George Street, Providence, RI, 02912				8. PERFORMING ORGANIZATION REPORT NUMBER	
9. SPONSORING/MONITORING AGENCY NAME(S) AND ADDRESS(ES)				10. SPONSOR/MONITOR'S ACRONYM(S)	
				11. SPONSOR/MONITOR'S REPORT NUMBER(S)	
12. DISTRIBUTION/AVAILABILITY STATEMENT Approved for public release; distribution unlimited					
13. SUPPLEMENTARY NOTES The original document contains color images.					
14. ABSTRACT					
15. SUBJECT TERMS					
16. SECURITY CLASSIFICATION OF:			17. LIMITATION OF ABSTRACT	18. NUMBER OF PAGES 21	19a. NAME OF RESPONSIBLE PERSON
a. REPORT unclassified	b. ABSTRACT unclassified	c. THIS PAGE unclassified			

1 Introduction

Most of the effort in CFD research so far has been in developing efficient algorithms for different applications, assuming an ideal input with precisely defined computational domains. With the field reaching now some degree of maturity, we naturally pose the more general question of how to model uncertainty and stochastic input, and how to formulate algorithms in order for the simulation output to reflect accurately the propagation of uncertainty. To this end, the Monte Carlo approach can be employed but it is computationally expensive and it is only used as the last resort. The sensitivity method is an alternative more economical approach, based on moments of samples, but it is less robust and it depends strongly on the modeling assumptions [1]. There are other more suitable methods for physical applications, and there has already been good progress in other fields, most notably in seismology and structural mechanics. A number of papers and books have been devoted to this subject, most notably with the work of Ghanem and others, e.g. [2, 3, 4, 5, 6, 7, 8, 9]. On the theoretical side, the work of Papanicolaou and his collaborators has addressed many aspects of wave propagation and other physical processes in random media, see for example [10].

An effective approach pioneered by Ghanem & Spanos [5] in the context of finite elements for solid mechanics is based on a spectral representation of the uncertainty. This allows high-order representation, not just first-order as in most perturbation-based methods, at high computational efficiency. It is based on the original ideas of Wiener (1938) on homogeneous chaos [11, 12] and the Hermite polynomials. The effectiveness of Hermite expansions was also recognized by Chorin (1971) [13] who employed Wiener-Hermite series to substantially improve both accuracy and computational efficiency of Monte Carlo algorithms. However, the limitation of prematurely truncated Wiener-Hermite expansions in applications of turbulence has also been diagnosed [14].

In this paper we consider the linear advection equation with a random transport velocity as a prototype problem, and as a first attempt to model uncertainty in propagation phenomena using polynomial chaos. The objective is to evaluate the Wiener-Hermite polynomial chaos in terms of its accuracy and efficiency. Given the simple equation considered, we are able to derive an exact solution for the mean and the variance of the stochastic solution. A new element in this paper is the representation of the stochastic input using Karhunen-Loève expansions both for a specified covariance kernel as well as a kernel constructed explicitly following a dynamical systems approach. In the simulations, we consider both Gaussian and log-normal distributions of the transport velocity. In the next sections, we first formulate the polynomial chaos algorithm, derive the exact solutions, and subsequently discuss different ways of input representation. We then present simulations with time- and space-dependent transport velocity, and

we conclude with a brief summary.

2 Polynomial Chaos: Wiener-Hermite Expansions

We consider the stochastic advection equation

$$\left\{ \begin{array}{l} \frac{\partial u}{\partial t} + V(x, t, \theta) \frac{\partial u}{\partial x} = 0 \quad \forall (t, x) \in [0, T] \times \mathcal{D} = [-1, 1] \\ u(t = 0, x) = g(x) \quad \forall x \in \mathcal{D} \\ \text{Periodic boundary conditions} \end{array} \right. \quad (1)$$

Here θ is a random parameter. We will examine cases with both time-independent as well as time-dependent transport velocity.

We first assume that the transport velocity $V(x, \theta)$ is only space-dependent and is a given random process with mean value and variance satisfying

$$\bar{V}(x) = E\{V(x, \theta)\} = 1 \quad \text{and} \quad E\{|V(x, \theta)|^2\} < \infty \quad (2)$$

where the covariance function

$$\mathcal{C}(x, y) = E\{V(x, \theta)\overline{V(y, \theta)}\} \quad (3)$$

is continuous. Its orthogonal decomposition is obtained by the Karhunen-Loève expansion

$$V(x, \theta) = \overline{V(x)} + \sum_{k=1}^M \sqrt{\lambda_k} f_k(x) \xi_k(\theta) = \sum_{k=0}^M g_k(x) \xi_k(\theta), \quad (4)$$

where ξ_k are Gaussian variables, and M is the *dimension*. The eigenvalues λ_k and corresponding eigenfunctions f_k satisfy the Helmholtz integral equation

$$\int_{\mathcal{D}} \mathcal{C}(x, y) f_k(y) dy = \lambda_k f_k(x). \quad (5)$$

By assuming that $u(t, x, \theta)$ is a second-order process, that is $u(t, x, \theta)$ has a finite variance, the theorem of Cameron & Martin [15] guarantees that the solution $u(t, x, \theta)$ can be represented in terms of polynomials, i.e.

$$\begin{aligned} u(t, x, \theta) = & a_0 \Gamma_0 + \sum_{i_1=1}^{\infty} a_{i_1} \Gamma_1(\xi_{i_1}(\theta)) + \sum_{i_1=1}^{\infty} \sum_{i_2=1}^{i_1} a_{i_1 i_2} \Gamma_2(\xi_{i_1}(\theta), \xi_{i_2}(\theta)) \\ & + \sum_{i_1=1}^{\infty} \sum_{i_2=1}^{i_1} \sum_{i_3=1}^{i_2} a_{i_1 i_2 i_3} \Gamma_3(\xi_{i_1}(\theta), \xi_{i_2}(\theta), \xi_{i_3}(\theta)) + \dots \end{aligned} \quad (6)$$

In the above equation, $\Gamma_n(\xi_{i_1}, \xi_{i_2}, \dots, \xi_{i_n})$ denotes the polynomial chaos of order n in the Gaussian variables $(\xi_{i_1}, \xi_{i_2}, \dots, \xi_{i_n})$.

The general expression for generating these polynomials is given by

$$\Gamma_n(\xi_{i_1}, \xi_{i_2}, \dots, \xi_{i_n}) = (-1)^n e^{\vec{\xi} \cdot \vec{\xi}^t / 2} \frac{\partial^n e^{-\vec{\xi} \cdot \vec{\xi}^t / 2}}{\partial \xi_{i_1} \partial \xi_{i_2} \dots \partial \xi_{i_n}} \quad (7)$$

where the vector $\vec{\xi}$ consisting of the n random variables $(\xi_{i_1}, \xi_{i_2}, \dots, \xi_{i_n})$.

Having equation (7), the decomposition in equation (6) can be thought of as

$$u(t, x, \theta) = \overbrace{a_0 \Gamma_0 + \sum_{i_1=1}^{\infty} a_{i_1} \Gamma_1(\xi_{i_1}(\theta))}^{\text{Gaussian part}} + \underbrace{\sum_{i_1=1}^{\infty} \sum_{i_2=1}^{i_1} a_{i_1 i_2} \Gamma_2(\xi_{i_1}(\theta), \xi_{i_2}(\theta)) + \sum_{i_1=1}^{\infty} \sum_{i_2=1}^{i_1} \sum_{i_3=1}^{i_2} a_{i_1 i_2 i_3} \Gamma_3(\xi_{i_1}(\theta), \xi_{i_2}(\theta), \xi_{i_3}(\theta)) + \dots}_{\text{non-Gaussian part}}$$

For a Gaussian process, only the first term is present and thus this expansion reduces to the Karhunen-Loève representation of the same process [16].

Equation (6) can be re-written in the more familiar form

$$u(t, x, \theta) = \sum_{i=0}^P \alpha_i(t, x) \Psi_i(\vec{\xi}(\theta)), \quad (8)$$

where there exists one-to-one correspondence between the $\Gamma_n(\xi_{i_1}, \xi_{i_2}, \dots, \xi_{i_n})$ and $\Psi_i(\vec{\xi}(\theta))$ as well as between the coefficients $\alpha_i(t, x)$ and a_{i_1, i_2, \dots, i_n} . The total number of polynomial chaoses ($P + 1$) used in the expansion is

$$\frac{(M + p)!}{M! p!},$$

where M and p refers to the dimension of the stochastic input and the order of the polynomial chaos, respectively.

In equation (8), $\alpha_i(t, x)$ are the deterministic coefficients and $\Psi_i(\vec{\xi}(\theta))$ is a trial basis in the space of random variables. This basis is the set of generalized multi-dimensional Hermite polynomials in the quantity $\vec{\xi}(\theta)$. This representation can be refined along the random dimension either by adding more random variables (dimension M) or by increasing the maximum order of polynomials included in the polynomial chaos expansion (order p).

If the solution is known, then the coefficients α_i in the expansion (8) can be obtained from

$$\alpha_i(t, x) = \frac{\langle u(t, x, \theta), \Psi_i(\vec{\xi}(\theta)) \rangle}{\langle \Psi_i(\vec{\xi}(\theta)), \Psi_i(\vec{\xi}(\theta)) \rangle}, \quad (9)$$

where

$$\langle \Psi_m(\vec{\xi}(\theta)), \Psi_n(\vec{\xi}(\theta)) \rangle = \int_{\Omega} \Psi_m(\vec{\xi}(\theta)) \Psi_n(\vec{\xi}(\theta)) dP \quad (10)$$

is the inner product (statistical average).

Substituting the above in the advection equation (1), it yields

$$\frac{\partial}{\partial t} \sum_{i=0}^P \alpha_i(t, x) \Psi_i(\vec{\xi}(\theta)) + \left(\sum_{j=0}^M \xi_j(\theta) g_j(x) \right) \frac{\partial}{\partial x} \sum_{i=0}^P \alpha_i(t, x) \Psi_i(\vec{\xi}(\theta)) = 0. \quad (11)$$

Assuming that we discretize in space with a spectral method we write

$$\alpha_i(x, t) = \sum_{k=0}^N \alpha_{ik}(t) \Phi_k(x) \quad (12)$$

where $\Phi_k(x)$ denotes the trial basis in space; here, we employ the Fourier exponentials, i.e. $\Phi_k(x) = e^{ikx}$. Upon substitution, we obtain

$$\sum_{i=0}^P \sum_{k=0}^N \frac{\partial \alpha_{ik}(t)}{\partial t} \Phi_k(x) \Psi_i(\vec{\xi}(\theta)) + \sum_{i=0}^P \sum_{j=0}^M \sum_{k=0}^N \xi_j(\theta) g_j(x) \Psi_i(\vec{\xi}(\theta)) \alpha_{ik}(t) \frac{\partial \Phi_k(x)}{\partial x} = 0. \quad (13)$$

We now apply a standard Galerkin projection, first in space x

$$\begin{aligned} & \sum_{i=0}^P \sum_{k=0}^N \frac{\partial \alpha_{ik}(t)}{\partial t} \Psi_i(\vec{\xi}(\theta)) \int_{\mathcal{D}} \Phi_k(x) \Phi_l(x) dx + \\ & \sum_{i=0}^P \sum_{j=0}^M \sum_{k=0}^N \xi_j(\theta) \Psi_i(\vec{\xi}(\theta)) \alpha_{ik}(t) \int_{\mathcal{D}} g_j(x) \frac{\partial \Phi_k(x)}{\partial x} \Phi_l(x) dx = 0 \end{aligned} \quad (14)$$

for $l = 0, 1, 2, \dots, N$

We denote by

$$I_{kl} = \int_{\mathcal{D}} \Phi_k(x) \Phi_l(x) dx$$

the mass matrix, and by

$$I_{jkl} = \int_{\mathcal{D}} g_j(x) \frac{\partial \Phi_k(x)}{\partial x} \Phi_l(x) dx,$$

the derivative matrix, to arrive at

$$\begin{aligned} & \sum_{i=0}^P \sum_{k=0}^N I_{kl} \frac{\partial \alpha_{ik}(t)}{\partial t} \Psi_i(\vec{\xi}(\theta)) + \sum_{i=0}^P \sum_{j=0}^M \sum_{k=0}^N I_{jkl} \alpha_{ik}(t) \xi_j(\theta) \Psi_i(\vec{\xi}(\theta)) = 0 \end{aligned} \quad (15)$$

for $l = 0, 1, 2, \dots, N$

By analogy with the deterministic approach, we use a Galerkin projection for the random variable as well, i.e. we multiply the system (15) by $\Psi_m(\vec{\xi}(\theta))$ and take the statistical average defined in equation (10). The orthogonality property of $\Psi_i(\vec{\xi}(\theta))$ is employed to arrive at

$$\begin{aligned} & \sum_{k=0}^N I_{kl} \frac{\partial \alpha_{mk}(t)}{\partial t} \langle \Psi_m \Psi_m \rangle + \sum_{i=0}^P \sum_{j=0}^M \sum_{k=0}^N I_{jkl} \alpha_{ik}(t) \langle \xi_j \Psi_i \Psi_m \rangle = 0 \end{aligned} \quad (16)$$

for $l = 0, 1, 2, \dots, N$ and $m = 0, 1, 2, \dots, P$

Once the coefficients α_{ik} have been evaluated, the stochastic solution can be obtained from

$$u(t, x, \theta) = \sum_{i=0}^P \sum_{k=0}^N \alpha_{ik}^n \Psi_m(\vec{\xi}(\theta)) \Phi_k(x), \quad (17)$$

where the superscript n here denotes time discretization.

We close the section by pointing out that the previous analysis remains unchanged in the case of $V(x, \theta)$ being a non-Gaussian process. In that case, the polynomial chaos expansion is used to represent the process instead of the Karhunen-Loève expansion. Consequently, the term $\langle \Psi_j \Psi_i \Psi_m \rangle$ replaces $\langle \xi_j \Psi_i \Psi_m \rangle$ in equation (16). A more general approach that involves different trial bases from the Askey scheme of orthogonal polynomials has been developed in [17].

3 Exact Stochastic Solutions

If the transport velocity V in equation (1) is a random function of the time t alone, the initial value problem can be solved exactly by the method of characteristics or by a change of variables. We demonstrate the latter method here.

We remove the random *positive* variable $V(t)$ from the equation by a change of variable t to τ as follows

$$\begin{cases} d\tau = V(t) dt \\ \tau = 0 \quad \text{when} \quad t = 0. \end{cases} \quad (18)$$

The advection equation (1) is then reduced to

$$\begin{cases} \frac{\partial u}{\partial \tau} + \frac{\partial u}{\partial x} = 0 \\ u(x, 0) = g(x). \end{cases} \quad (19)$$

The solution to the above equation is simply given by

$$u(x, t) = g(x - \tau), \quad (20)$$

while the solution for τ is obtained by solving equation (18)

$$\tau(t) = \int_0^t V(s) ds = \Delta t \sum_{j=1}^Q v_j. \quad (21)$$

In order to evaluate the sum of the set of random variables v_j in (21), we assume v_j to be

$$\begin{cases} v_1 = a\xi_1 \\ v_i = cv_{i-1} + af\xi_i \quad \text{for} \quad i = 2, 3, \dots, Q \end{cases} \quad (22)$$

where a, c determine the degree of correlation of the input, and $f^2 = 1 - c^2$ to ensure that each v_i has the same variance a . Also, $\xi_1, \xi_2, \dots, \xi_Q$ are a set of independent normal random variables of variance unity, i.e.,

$$\xi_i = \frac{1}{\sqrt{2\pi}} e^{-\frac{\xi^2}{2}} \quad \forall i = 1, 2, \dots, Q \quad (23)$$

We obtain the following three cases :

Case I - Fully Correlated Input: For $c = 1$ and $f = 0$ the input is fully correlated, and

$$\sum_{j=1}^Q v_j = aQ\xi_1 = aQ\xi$$

Case II - Mutually Independent: For $c = 0$ and $f = 1$ the input is mutually independent, and

$$\sum_{j=1}^Q v_j = a\sqrt{Q}\xi$$

Case III- Partially Correlated Input:: For general values of c , we obtain

$$\sum_{j=1}^Q v_j = a \left[\frac{1+c}{1-c} Q - \frac{2c}{(1-c)^2} (1-c^Q) \right]^{1/2} \xi.$$

Letting $t = Q\Delta t$, we obtain

$$\tau(t) = \Delta t \sum_{j=1}^Q v_j = \begin{cases} at\xi + \bar{V}t \\ a\sqrt{t\Delta t}\xi + \bar{V}t \\ a[2At - 2A^2(1 - e^{-t/A})]^{1/2}\xi + \bar{V}t \text{ as } (c \rightarrow 1, \Delta t \rightarrow 0) \end{cases} \quad (24)$$

We can now write the solution to equation(20) as

$$u(x, t) = u(x, \tau(t)) = g(x - \tau(t)) \quad (25)$$

and obtain its mean by taking the expectation value of equation (25) with the normal distribution (23):

$$\bar{u}(x, t) = \frac{1}{\sqrt{2\pi}a\sigma} \int_{-\infty}^{\infty} g(x_0) e^{-\frac{(x - x_0 - \bar{V}t)^2}{2a^2\sigma^2}} dx_0 = \sin \pi(x + 1 - \bar{V}t) e^{-\pi^2\sigma^2 a^2/2}, \quad (26)$$

where σ is defined from

$$\sigma^2 = \begin{cases} t^2 & \text{for fully correlated case} \\ (\Delta t)t & \text{for mutually independent case} \\ 2A[t - A(1 - e^{-t/A})] & \text{for partially correlated case} \end{cases} \quad (27)$$

The variance of the random variable $u(x, t)$ is obtained from

$$\text{Var}(u) = E\{u^2\} - \bar{u}^2,$$

which together with the normal distribution (23) yields

$$\text{Var}(u(x, t)) = \frac{1}{2}[1 - \cos 2\pi(x - \bar{V}t)e^{-2(\pi a\sigma)^2}] - \bar{u}^2 = \frac{1}{2}(1 - e^{-\pi^2\sigma^2 a^2})[1 + \cos 2\pi(x + 1 - \bar{V}t)e^{-\pi^2\sigma^2 a^2}], \quad (28)$$

where $g(x_0)$ was set to $\sin \pi(x_0 + 1)$ in order to obtain equation (28).

4 Representation of Stochastic Inputs

We consider different representations of the stochastic inputs corresponding to covariance kernels specified or constructed explicitly following a dynamical systems approach.

4.1 Specified Covariance Kernels

In the case of time-dependent but space-independent transport velocity, i.e.

$$V(t, x, \omega) = V(t, \omega)$$

we use the **exponential kernel**

$$\mathcal{C}(t, s) = \exp\left\{-\frac{|t-s|}{b}\right\},$$

where b is a parameter which has the same dimension as time t and is termed *correlation length*. It expresses the rate at which the correlation decays between two time instants of the process. For the kernel under consideration, the analytical solution to the integral equation (5) can be found in the following fashion:

Let $\mathcal{T} = [0, T]$ where T designate the final time, and set $c = \frac{1}{b}$. The integral equation (5) becomes

$$\int_0^T e^{-c|t-s|} f_k(s) ds = \lambda_k f_k(t), \quad (29)$$

which can be written as

$$\int_0^t e^{-c(t-s)} f_k(s) ds + \int_t^T e^{c(t-s)} f_k(s) ds = \lambda_k f_k(t), \quad (30)$$

Since the integrands in (30) are continuous, differentiating (30) twice with respect to t yields

$$\lambda \ddot{f}(t) = (-2c + c^2 \lambda) f(t), \quad (31)$$

where the subscript k was omitted. The boundary conditions associated with (31) are

$$\begin{cases} \dot{f}(0) - cf(0) = 0 \\ \dot{f}(T) + cf(T) = 0 \end{cases} \quad (32)$$

Making the substitution

$$\omega^2 = \frac{2c - c^2\lambda}{\lambda}, \quad (33)$$

the boundary value problem

$$\begin{cases} \ddot{f}(t) + \omega^2 f(t) = 0 \\ \dot{f}(0) - cf(0) = 0 \\ \dot{f}(T) + cf(T) = 0 \end{cases} \quad (34)$$

follows. Solutions to (34) are given by

$$f(t) = \alpha \cos(\omega t) + \beta \sin(\omega t), \quad (35)$$

with dispersion relation

$$(\omega^2 - c^2) \tan \omega T - 2c\omega = 0, \quad (36)$$

from which ω can be determined. The normalized eigenfunctions are

$$f(t) = \frac{\frac{\omega}{c} \cos(\omega t) + \sin(\omega t)}{\sqrt{\frac{1}{2} \left(1 + \frac{\omega^2}{c^2}\right) T + \left(\frac{\omega^2}{c^2} - 1\right) \frac{\sin(2\omega T)}{4\omega} + \frac{1}{2c} (1 - \cos(2\omega T))}} \quad (37)$$

When the transport velocity is space-dependent,

$$V(t, x, \omega) = V(x, \omega)$$

we use a similar kernel of the form employed by Ghanem & Spanos [18]

$$\mathcal{C}(x, y) = \exp\left\{-\frac{|x - y|}{b}\right\}$$

A similar analysis as before produces analytical forms for the eigenvalues and eigenfunctions.

4.2 Dynamical Systems Approach

We also consider different ways for correlations to represent stochastic inputs, which can be useful to represent discrete input. Specifically, we consider the following two processes:

$$u_k = cu_{k-1} + af\xi_k, \quad (38)$$

$$u_k = \frac{c}{2}(u_{k+1} + u_{k-1}) + af\xi_k. \quad (39)$$

The first process (38) is autoregressive of order 1 and corresponds to the Markov process. The second process is termed bilateral autoregressive process due to its backward and forward dependence. The constant c is assumed to be $0 \leq c \leq 1$ in order to ensure that the processes is of finite variance. Here, ξ_k is a random variable of mean zero and variance one, and f is a constant to be determined such that for the given values of a and c the variance of the process is equal to a^2 .

We can construct numerically the covariance kernel and subsequently extract the eigenvalues and eigenfunctions needed for the input. Alternatively, we can write

$$u_k = \sum_{i=1}^{N-k+1} \alpha_i \xi_{k+i-1} + \sum_{i=N-k+2}^N \alpha_i \xi_{N-k+1} \quad (40)$$

and solve for α_i . A simple calculation based on projection and orthogonality of the Gaussian random variable ξ_i yields the following expression for the mean value

$$E\{u_i u_j\} = \sum_{k=1}^{N-|i-j|} \alpha_k \alpha_{k+|i-j|} + \sum_{k=1}^{|i-j|} \alpha_k \alpha_{N-(|i-j|-k)}. \quad (41)$$

In figures 1 and 2 we give the eigenfunctions and compare the eigenspectra between a unilateral and a bilateral autoregressive process. Periodic boundary conditions were assumed for these calculations.

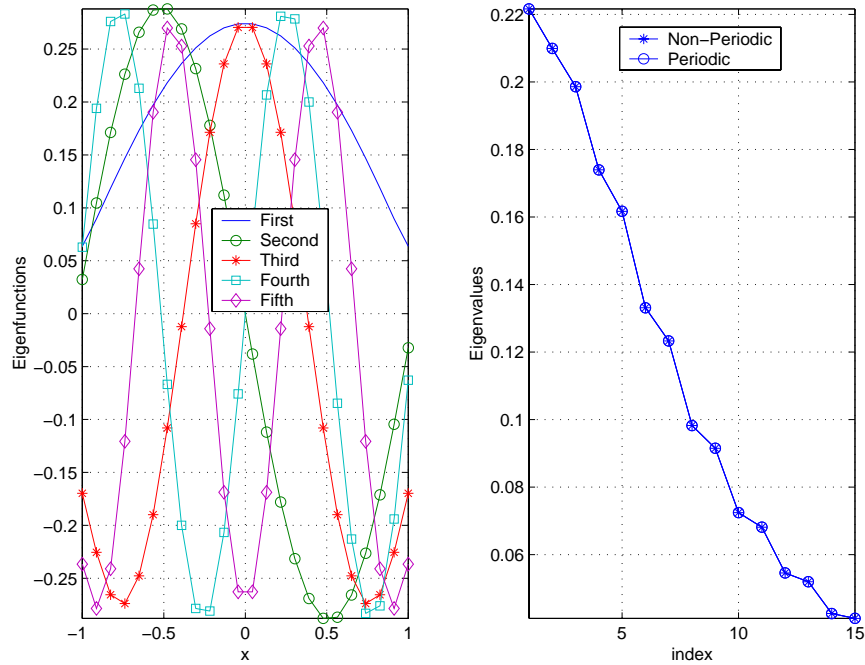


Figure 1: Eigenfunctions and eigenspectra corresponding to $c = 0.5$ and $a = 1$.

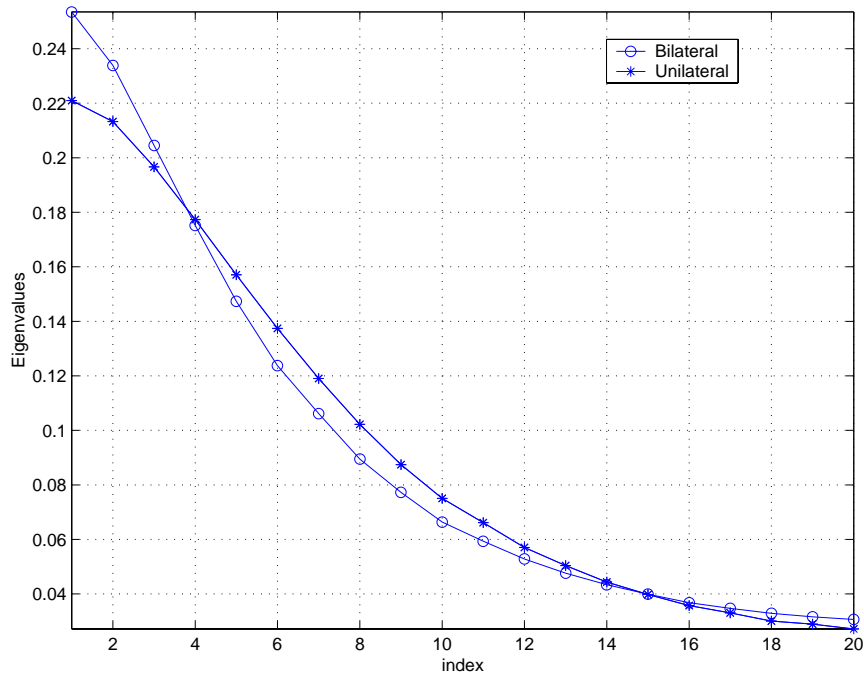


Figure 2: Comparison between unilateral and bilateral eigenspectra.

5 Numerical Results

We consider the stochastic advection equation with initial condition

$$g(x) = \sin \pi(1 + x) \quad x \in [-1, 1].$$

In the following we use Fourier collocation to treat the deterministic contributions. We also perform Monte Carlo simulations to compare with the polynomial chaos results. For the latter we found it necessary to use a Lagrangian approach in solving the stochastic advection equation. That is, we have implemented a solution based on characteristics that avoids global spectral interpolation. In contrast, following an Eulerian approach leads to erroneous results due to the lack of smoothness in the stochastic solution. Specifically, the Lagrangian and Eulerian numerical solutions are initially very close to each other but for longer time integration errors in the Eulerian approach render the solution erroneous.

In the following, we consider several cases corresponding to different types of stochastic input representation. We employ both *ad hoc* type covariance kernels as well as kernels constructed based on a dynamical systems approach.

5.1 Space-Independent Transport Velocity

First, we assume that $V(t, x, \theta) \equiv V(t, \theta)$ and employ the kernel

$$C(s, t) = \exp\left\{-\frac{|t-s|}{b}\right\}$$

for the covariance matrix. We also perform a companion Monte Carlo simulation; this kernel corresponds to a unilateral autoregressive process, as defined previously. For comparisons, we also obtain the analytical mean solution and variance.

For the **fully correlated case**, figures 3 and 4 show the results for the mean and variance, respectively. Good agreement between the solution obtained from the polynomial chaos simulation, the Monte Carlo simulation, and the exact formulas is obtained.

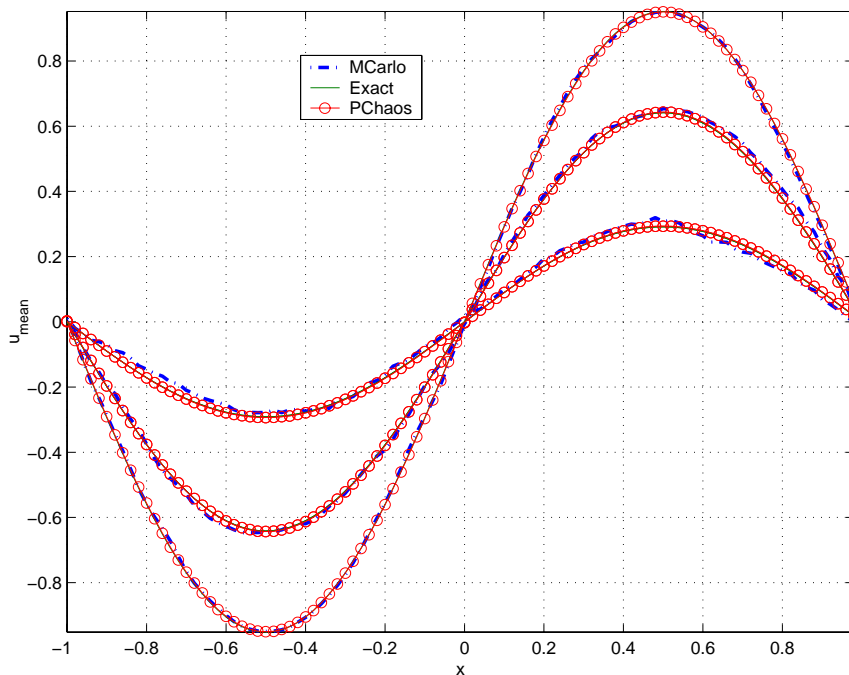


Figure 3: Mean solutions for the *fully correlated* case, after $t = 1$, $t = 3$ and $t = 5$. The mean solution decays exponentially with time.

For the **partially correlated** case and the **mutually independent** case similar conclusions to the fully correlated case can be drawn. Indeed, as shown by the figures 5 and 6, also figures 7 and 8, good agreement between polynomial chaos simulation, Monte Carlo and exact formulas is established for both mean and variance. It is worth mentioning that in the case of partial correlation, up to $M = 6$ stochastic dimensions were required for the polynomial chaos simulation in order to agree with the exact formula.

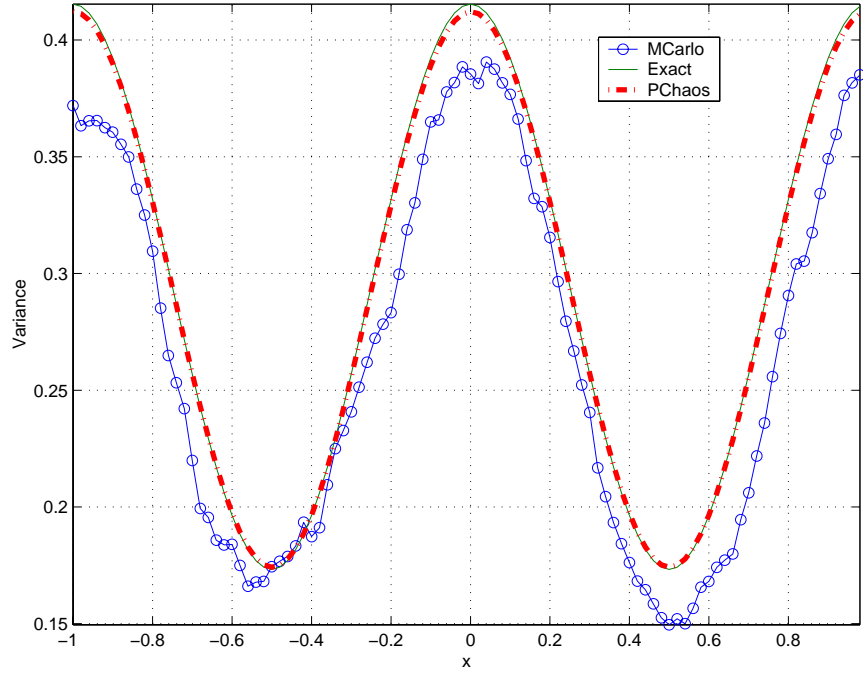


Figure 4: Variance of the solution for the *fully correlated* case, after $t = 3$.

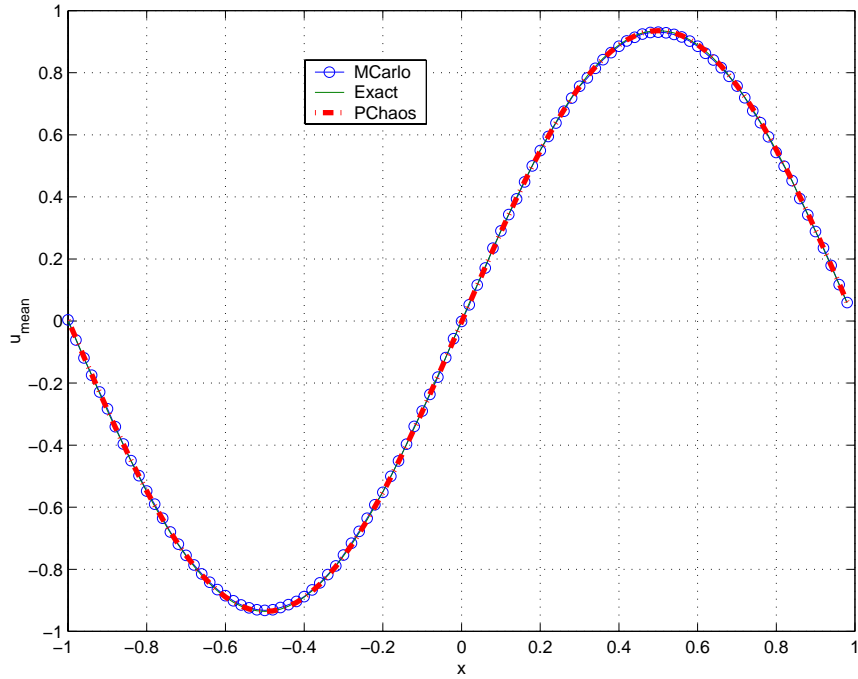


Figure 5: Mean solution for the *partially correlated* case, $c = 0.5$, after $t = 5$; $M = 6$ and $p = 4$.

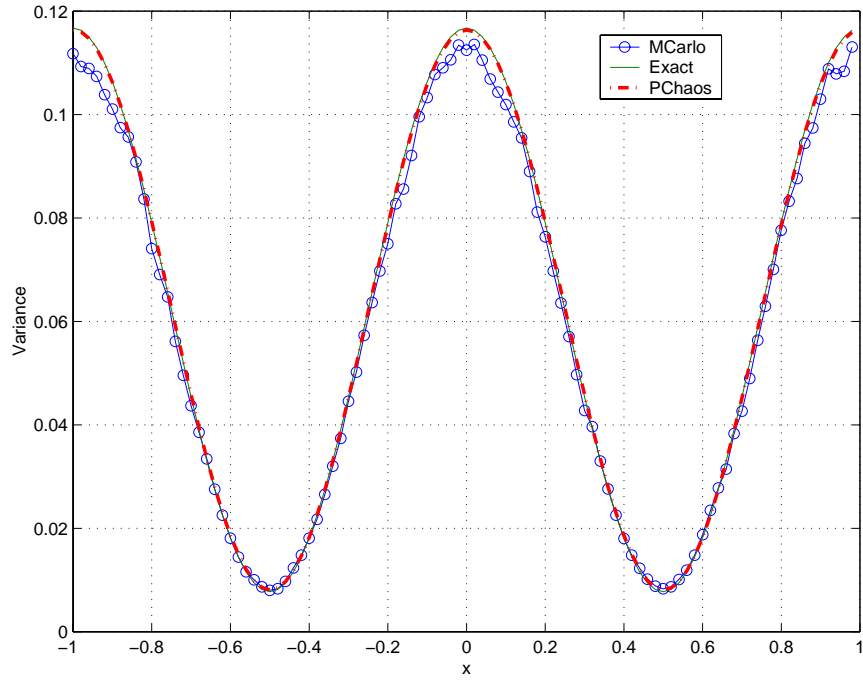


Figure 6: Variance of the solution for the *partially correlated* case, $c = 0.5$, after $t = 5$; $M = 6$ and $p = 4$.

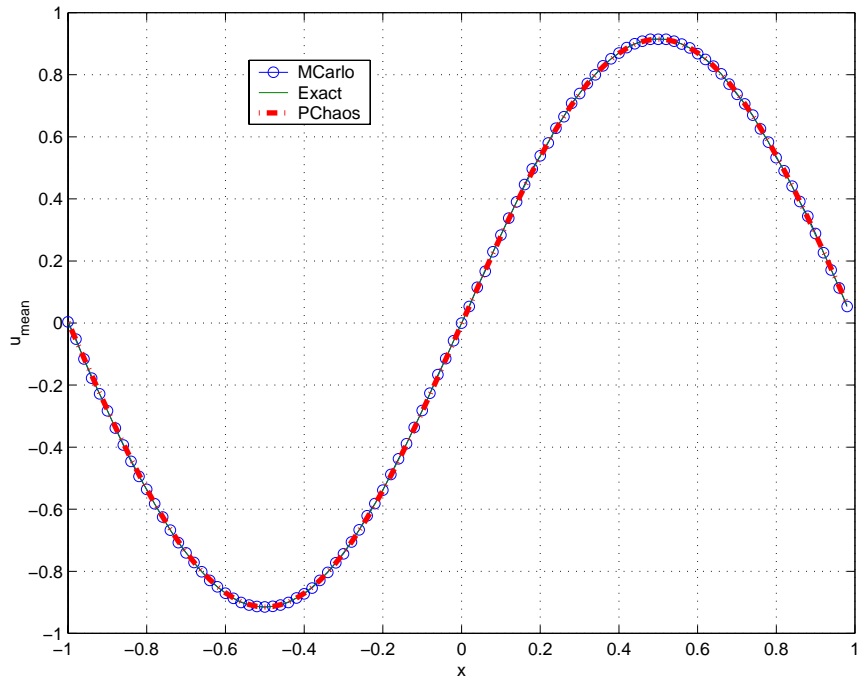


Figure 7: Mean solution for the *mutually independent* case, c approaches 0, after $t = 3$; $M = 2$ and $p = 4$.

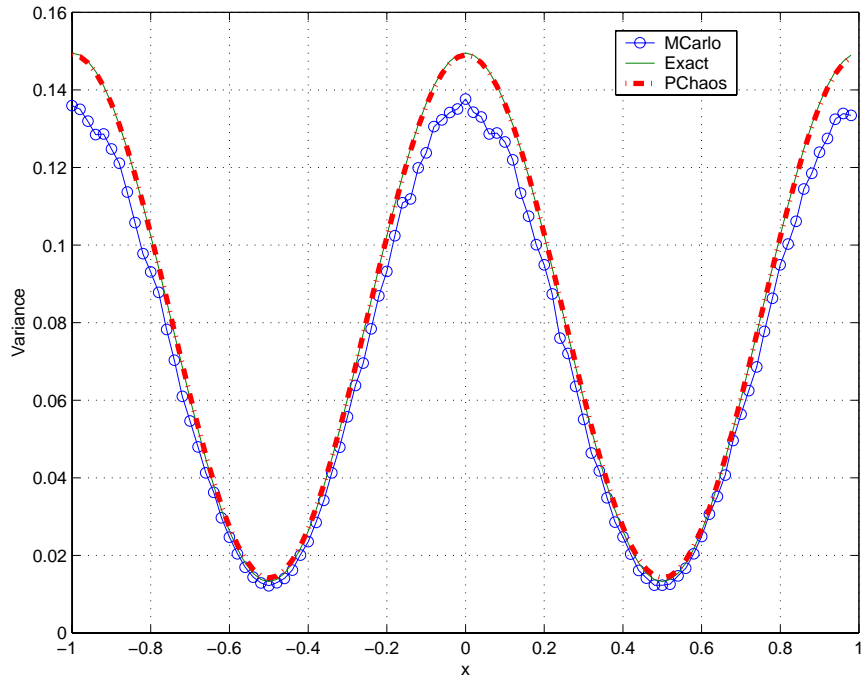


Figure 8: Variance of the solution for the *mutually independent* case, c approaches 0, after $t = 3$; $M = 2$ and $p = 4$.

5.2 Time-Independent Transport Velocity

We replace now the transport velocity $V(t, x, \theta)$ by $V(x, \theta)$ and assume that the stochastic transport velocity is represented by the covariance matrix

$$\mathcal{C}(x, y) = \exp\left\{-\frac{|x - y|}{A}\right\}.$$

An algorithm similar to the one used for time-dependent transport velocity was employed. For a length scale of $A = 1$, for the fully-correlated case after a time of $t = 1$ we observed that the mean solution diverges. The cause is attributed to the non-periodicity of the specified exponential kernel. To circumvent this difficulty, we constructed a periodic covariance kernel, generated numerically as discussed in section 3; see figure 9.

We obtain the results presented in figures 10 and 11, after integrating to time $t = 10$. Here again agreement between polynomial chaos and Monte Carlo simulation of 50,000 realizations is established.

5.3 Non-Gaussian Input

Lastly, we consider a case where the transport velocity is not Gaussian, but is given by the log-normal distribution

$$V(x, \theta) = e^h, \quad h = \bar{h} + \sum_{l=1}^L h_l \xi_l$$

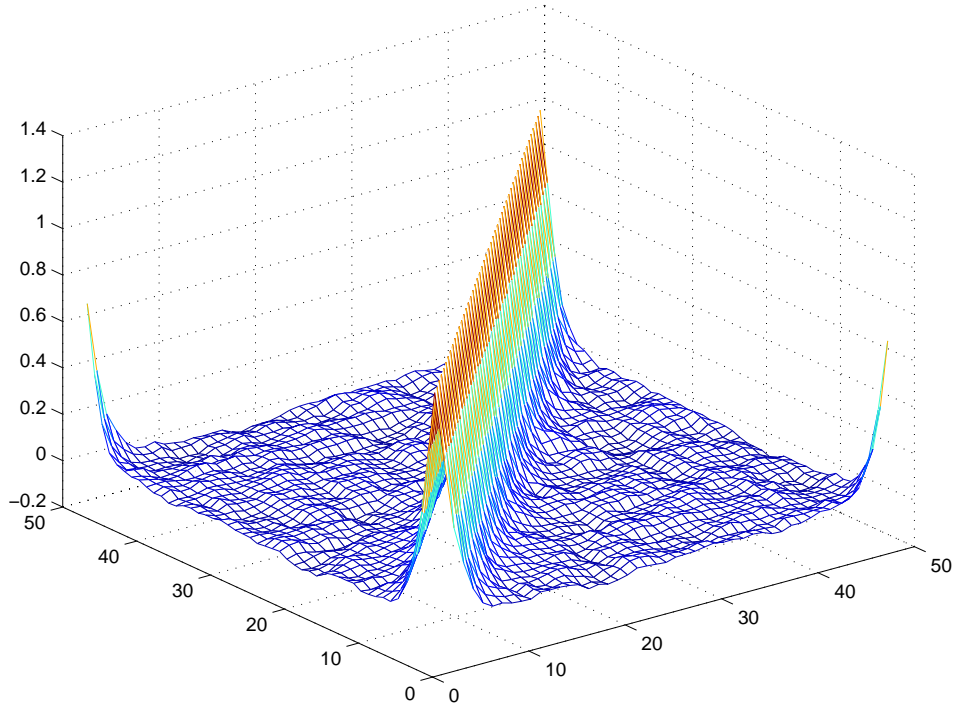


Figure 9: Numerically generated covariance kernel for periodic boundary conditions, $c = 0.5$.

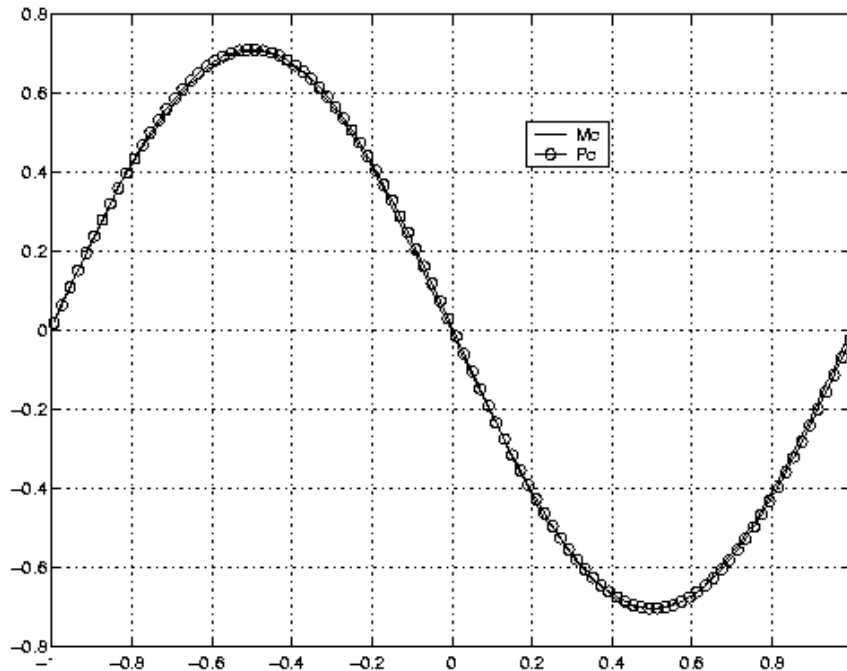


Figure 10: Time-independent case: Mean velocity after $t = 10$.

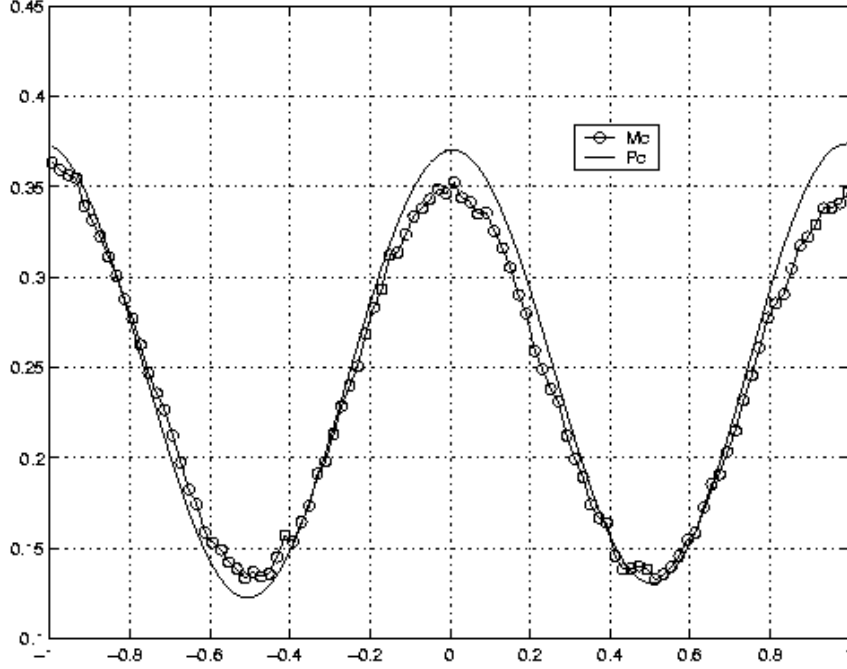


Figure 11: Time-independent case: Variance after $t = 10$.

In order to preserve the mean value of V , which was set to unity in the previous examples, the coefficients in the above equations have to be chosen according to the relation

$$\bar{h} + \frac{\sum_{l=1}^N h_l^2}{2} = 0.$$

For $\bar{h} = 0$ and h_l small enough, we recover the Gaussian case by using a Taylor expansion for e^h . The discrete stochastic advection equation is now

$$\frac{\partial \alpha_k^N}{\partial t} + \sum_{i=0}^P \sum_{j=0}^L \frac{\langle \Psi_i \Psi_j \Psi_k \rangle \langle \Psi_j(\boldsymbol{\eta}) \rangle}{\langle \Psi_j^2 \rangle \langle \Psi_k^2 \rangle} \exp\left\{\bar{h} + \frac{\sum_{l=1}^N h_l^2}{2}\right\} \frac{\partial \alpha_i^N}{\partial x} \Big|_{x=x_n} = 0 \quad (42)$$

$$\forall k = 0, 1, 2, \dots, P \text{ and } \forall n = 0, 1, 2, \dots, N - 1$$

In figures 12 and 13 we show a typical result for the mean solution and the variance, respectively, obtained at $t = 1.5$. A Monte Carlo simulation consisting of 20,000 realizations, is included to compare between the results obtained by both methods as there is no exact solution available for this case. The accuracy of the approximation in the mean is higher than in the variance but overall similar conclusions are valid for the lognormal distribution as well. In [17] a more systematic study for several different distribution functions is performed, and appropriate orthogonal polynomial functionals are introduced as trial basis.

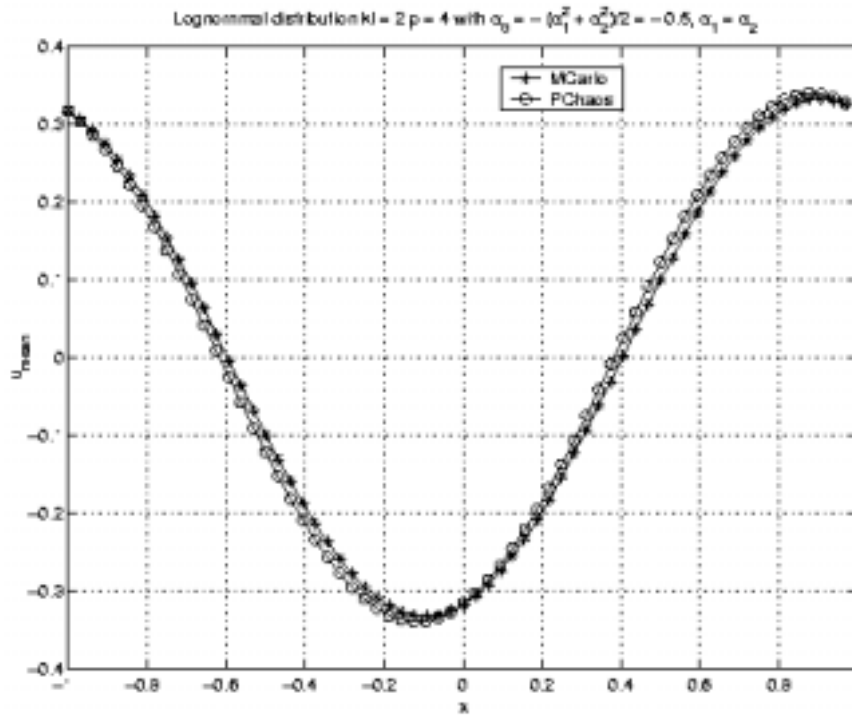


Figure 12: Lognormal distribution *mean solution* corresponding to $h_1 = h_2$ and $\bar{h} = -0.5$ after $t = 1.5$

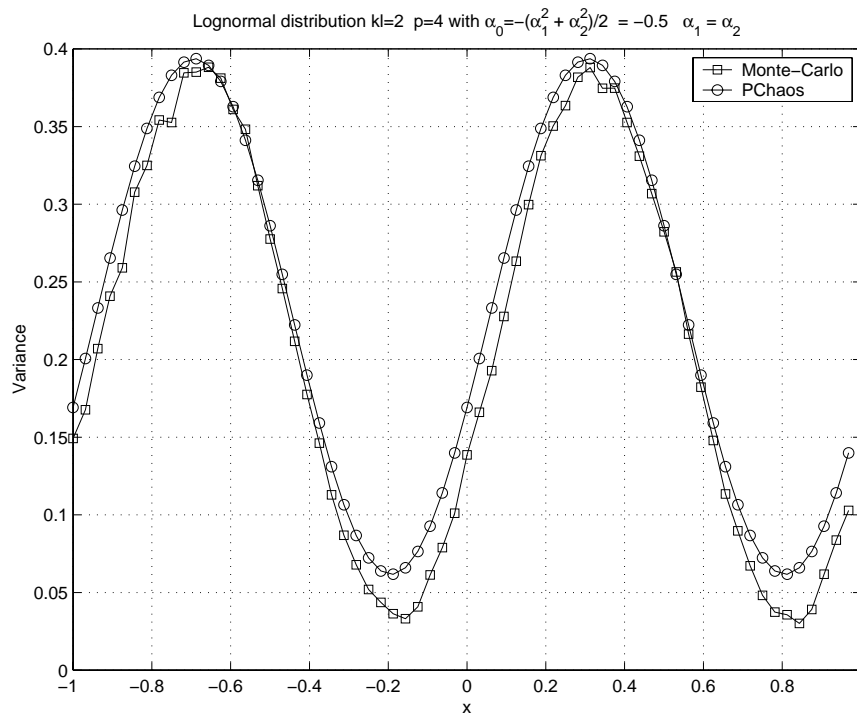


Figure 13: Lognormal distribution *variance* corresponding to $h_1 = h_2$ and $\bar{h} = -0.5$ after $t = 1.5$

6 Summary

We have developed a stochastic spectral method to solve the advection equation with a transport velocity described by a Gaussian or a log-normal distribution. It employs Wiener-Hermite functionals, which are Hermite polynomials of a Gaussian random variable ξ , which in turn depends on a random parameter θ . More general distributions can also be handled with Wiener-Hermite expansions but we have found in ongoing work [17] that better representations with other trial bases from the Askey scheme of polynomials lead to faster convergence compared to Hermite expansions.

The Wiener-Hermite expansion exhibits exponential convergence, which we verified for the space-independent case for which an exact solution was obtained. To realize exponential convergence the stochastic input has to be accurately represented but this depends on the correlation length of the stochastic input. In the case of poorly correlated input a very large number of Karhunen-Loève terms are required to represent the input and fast convergence is not achievable. The relatively poor resolution properties of Hermite expansions, compared to other spectral polynomials, are well documented in the literature [19, 20]. However, re-scaling procedures, as done in [21], can be applied or a change of the trial basis from the Askey scheme can be employed, as demonstrated in [17], to accelerate convergence. Unfortunately, the exact resolution requirements are problem-dependent and there is not enough experience at the moment in order to come up with practical rules.

As regards efficiency, we have compared with corresponding Monte Carlo simulations. Again, for the exact solution the standard Monte Carlo approach we employed requires 200,000 realizations to achieve errors in the mean solution of order of 10^{-2} . The same accuracy can be achieved with a 10-term polynomial expansion leading to a speed-up factor of 20,000. Clearly, better Monte Carlo approaches with accelerated convergence may reduce that speed-up but it will still be more than a factor of 1,000. However, as we discussed above, for stochastic input that is very weakly correlated the polynomial chaos approach requires a Karhunen-Loève expansion with many terms. This may increase significantly the dimensionality and thus the computational complexity of the polynomial chaos approach.

Acknowledgements

This work was supported by DOE and ONR.

References

- [1] R.G. Hills and T.G. Trucano. Statistical validation of engineering and scientific models: Background. Technical Report SAND99-1256, Sandia National Laboratories, 1999.
- [2] R.G. Ghanem. Stochastic finite elements for heterogeneous media with multiple random non-Gaussian properties. *ASCE J. Eng. Mech.*, 125(1):26–40, 1999.
- [3] R.G. Ghanem. Ingredients for a general purpose stochastic finite element formulation. *Comp. Meth. Appl. Mech. Eng.*, 168:19–34, 1999.
- [4] T.D. Fadale and A.F. Emery. Transient effects of uncertainties on the sensitivities of temperatures and heat fluxes using stochastic finite elements. *J. Heat Trans.*, 116:808–814, 1994.
- [5] R.G. Ghanem and P. Spanos. *Stochastic finite elements: a spectral approach*. Springer-Verlag, 1991.
- [6] W.K. Liu, G. Besterfield, and A. Mani. Probabilistic finite elements in nonlinear structural dynamics. *Comp. Meth. Appl. Mech. Eng.*, 56:61–81, 1986.
- [7] W.K. Liu, A. Mani, and T. Belytschko. Finite element methods in probabilistic mechanics. *Probabilistic Eng. Mech.*, 2(4):201–213, 1987.
- [8] M. Shinozuka and E. Leone. A probabilistic model for spatial distribution of material properties. *Eng. Fracture Mech.*, 8:217–227, 1976.
- [9] M. Shinozuka. Structural response variability. *J. Eng. Mech.*, 113(6):825–842, 1987.
- [10] L. Ryzhik, G. Papanicolaou, and J.B. Keller. Transport equations for elastic and other waves in random media. *Wave Motion*, 24:327–370, 1996.
- [11] N. Wiener. The homogeneous chaos. *Amer. J. Math.*, 60:897–936, 1938.
- [12] N. Wiener. *Nonlinear problems in random theory*. MIT Technology Press and John Wiley and Sons, New York, 1958.
- [13] A.J. Chorin. Hermite expansion in Monte-Carlo simulations. *J. Comput. Phys.*, 8:472–482, 1971.
- [14] S.A. Orszag and L.R. Bissonnette. Dynamical properties of truncated Wiener-Hermite expansions. *Phys. Fluids*, 10:2603, 1967.

- [15] R.H. Cameron and W.T. Martin. The orthogonal development of nonlinear functionals in series of Fourier-Hermite functionals. *Ann. of Math.*, 48:385, 1947.
- [16] M. Loève. *Probability theory, Fourth edition*. Springer-Verlag, 1977.
- [17] D. Xiu and G.E. Karniadakis. Modeling uncertainty in flow simulations via generalized polynomial chaos. *J. Comp. Phys.*, to appear, 2001.
- [18] P. Spanos and R.G. Ghanem. Stochastic finite element expansion for random media. *ASCE J. Eng. Mech.*, 115(5):1035–1053, 1989.
- [19] D. Gottlieb and S.A. Orszag. *Numerical Analysis of Spectral Methods: Theory and Applications*. CBMS-NSF, SIAM, Philadelphia, PA, 1977.
- [20] J.P. Boyd. The rate of convergence of Hermite function series. *Math. Comp.*, 35:1039–1316, 1980.
- [21] T. Tang. The Hermite spectral methods for Gaussian-type functions. *SIAM J. Sci. Comp.*, 14:594–606, 1993.